INL/CON-16-39097
PREPRINT

Reducing Demand Charges and Onsite Generation Variability Using Behind-the-Meter Energy Storage

IEEE Technology for Sustainability (SusTech) 2016

Bishnu P. Bhattarai, Kurt S. Myers, Jason W. Bush

April 2017

The INL is a
U.S. Department of Energy
National Laboratory
operated by
Battelle Energy Alliance

Reducing Demand Charges and Onsite Generation Variability Using Behind-the-Meter Energy Storage

Bishnu P. Bhattarai, *Member, IEEE*, Kurt S. Myers, *Member, IEEE*, and Jason W. Bush
Department of Power and Energy Systems
Idaho National Laboratory
Idaho Falls, Idaho, USA.
Emails: {*bishnu.bhattarai, kurt.myers, jason.bush*}*@inl.gov*

***Abstract*—Electric utilities in the United States are increasingly employing demand charges and/or real-time pricing. Such directive is bringing potential opportunities in deploying behind-the-meter energy storage (BMES) systems for various grid applications. This study quantifies the techno-economic benefits of BMES in reducing demand charge and smoothing load/generation intermittencies, and determines how those benefits vary with different penetration of onsite photovoltaic. We proposed a two-stage control algorithm, whereby the first stage proactively determines the cost-optimal BMES configuration for reducing peak demands and demand charges and the second stage adaptively compensates intermittent generations and short load spikes that may otherwise increase the demand charges. The performance of the proposed algorithm is evaluated through a 24-hours time sweep simulation performed using data from a smart microgrid testbed at Idaho National Laboratory. The simulation results demonstrated that this research provides a simple and effective solution for peak shaving, demand charge reductions, and onsite photovoltaic variability smoothing.**

***Keywords*—Behind-the-meter, demand charges, energy storage, microgrid, onsite generation, two-stage control.**

I. Background

Increased penetration of intermittent renewable energy sources (RESs) creates various control and operational challenges to the existing grid. Due to increasing availability of behind-the-meter energy storage (BMES), it can serve as one of the potential solutions not only to address those grid issues but also to optimally utilize onsite photovoltaic (PV) generation [1]. In particular, BMES has massive untapped potential that alone can cover a huge percentage of contemporary storage requirements. For example, BMES in California has 1,000 megawatts of capacity, which is equivalent to three-quarters of California's 2020 energy storage mandate [2]. However, one of the potential barriers to exploit BMES is its trivial economic benefits to BMES customers compared to the huge investment requirement. Such scenario provides significant but challenging opportunities to the research community for making BMES technically and economically viable solution for providing multiple grid services.

Electric utilities in the United States are recently making favorable policies and tariff structures for BMES owners in an effort to effectively exploit currently untapped BMES potential. On the other hand, research communities have also been extensively investing efforts in deploying BMES for multiple grid applications, such as ensuring energy security, improving system reliability, providing ancillary services, and reducing utility upgrade costs, demand charges, and peak demands. For instance, the authors in [3] presented an algorithm to utilize lithium-ion battery energy storage for peak shaving, while the authors in [4]-[6] developed control strategies for utilizing thermal and electrical energy storage for various grid functionality. Control strategies for utilizing battery storage and demand response for local grid constraints violation management are presented in [7]-[10]. Similarly, the use of energy storage for dynamic energy management and frequency regulation are presented in [11]-[12]. Despite those technically attractive solutions for deploying BMES for different grid services, the economic viability of BMES is often not justified. Demand charge reduction is one of the key BMES applications that can directly leverage economic benefits to BMES users [12].

In order to increase the economic benefits of storage, authors in [13]-[14] presented a two-stage procedure, whereby the optimum storage size for the given system is made as a part of planning decision and the optimum operational strategy is developed to maximize the benefits out of the given storage size. Similarly, adaptive and near-optimal control strategy for energy storage is presented in [15]-[17] to maximize the benefits of onsite PV generation. The strategies to exploit energy storage combined with the onsite RES generation are further developed in [18]-[19]. Most of the existing literature compute BMES benefits using deterministic models, whereby consumers are assumed to be aware in advance of their energy consumptions pattern [19]. However, load spikes and onsite RES variability make the use of those models very challenging and less effective in reducing demand charges. As many electric utilities are currently looking for a techno-economically attractive solution for integrated deployment of BMES and high penetrations of onsite PVs, it is of utmost importance to have an approach that is capable of addressing the high uncertainties stemming from intermittent renewables.

This study has developed a multi-timescale control framework to reduce demand charges and effectively address RES generation uncertainties. In particular, we proposed a two-stage control, whereby the first stage is 15 minutes resolution based control designed to proactively determine a cost-optimal BMES configuration for reducing peak demands and demand charges. Any uncertainties stemming from generation variability and load spikes in near real-time operation are smoothed out by the second adaptive control stage. Such different time-

This research was supported by Idaho National Laboratory WFO and Laboratory-Directed Research and Development projects.

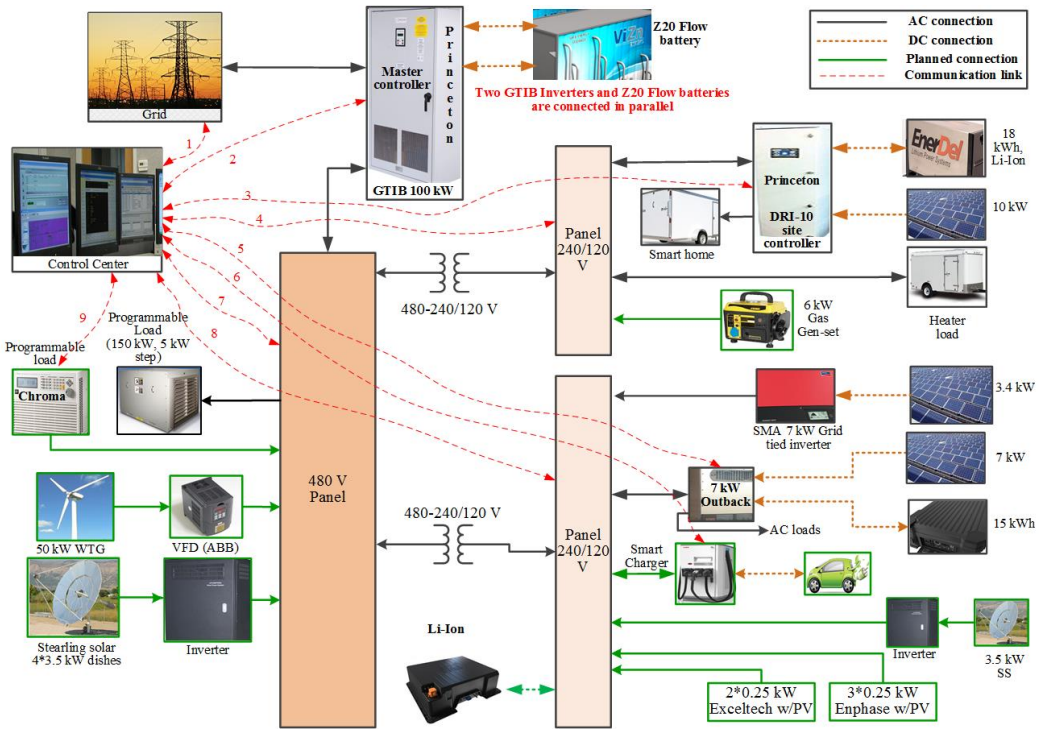

Fig. 1. Overall schematic diagram of test system (Microgrid Testbed at INL).

resolution-based control scheme provides an opportunity to deploy BMES for multiple grid service, including demand charge reduction, load leveling, and onsite PV variability smoothing, thereby ensuring the economic benefits to the BMES owner as well as technical benefits to the grid operators.

The remainder of the paper is structured as follows. First, the details of the system modeling are presented in Section II. In Section III, the multi-timescale control algorithm designed to realize demand charge reduction and smoothing onsite PV variability is presented. Details of the simulation configuration and results are presented in Section IV. Finally, the paper is concluded in Section V.

II. Test System Modeling

A smart microgrid testbed (MGT) at Idaho National Laboratory is primarily used as a test network. As shown in Fig. 1, MGT primarily comprises BMES, onsite PV generation, controllable load, and a combination of centralized and decentralized control architecture. The testbed includes a total of 21 kW PV systems, two flow batteries each having 64 kW, 160 kWh, a lead-acid battery (15 kWh), two grid-tied inverter and battery controllers (GTIB 100), a demand response inverter (DRI 10), a controllable load (150 kW), and a smart home comprising various household appliances (e.g., electric water heater, smart thermostat, computers, and lights). Moreover, a heterogeneous mesh communication network comprising Ethernet, power line carrier, and Wi-Fi is integrated to facilitate data acquisition and control of each microgrid component. The following subsections present modeling of key MGT components, including solar PV, BMES, and base loads.

A. PV System Model

We developed a simplified model of a grid-tied PV system, whereby the PV system is modeled as a dispatchable static generator that is capable of operating as a constant power source at the dispatched active and reactive power (PQ) set points. The PQ capability curve of the PV system is designed as shown in Fig. 2 in compliance with IEEE 1547 standards for distributed energy resources $\leq$ 30 kW capacity to keep the power factor (PF) of the PV inverter 0.85 lead/lag or higher. The control scheme of the grid-tied inverter is designed such that the active power is mostly limited by the available solar irradiance, while the reactive power limit is set per the IEEE 1547 standard to keep the PF within predefined limits. It is worth mentioning that, the reactive power injection/absorption is zero as long as the voltage at the point of common coupling (PCC) is within the acceptable limit and/or there is no dispatch request from the upstream control centers/grid operators. In either case, the reactive power injection from the grid-tied PV is limited by $\pm$ 0.85 PF.

B. Load Model

Loads are modeled using a generic ZIP approach, whereby the actual load consumption is expressed as an algebric sum of constant power, constant current, and constant impedance loads. The active and reactive power consumption of the loads are expressed in terms of voltage and ZIP coefficients as:

$$\begin{aligned} P &= P_0 \left(\alpha_1^P \cdot (\frac{V}{V_0})^2 + \alpha_2^P \cdot (\frac{V}{V_0}) + \alpha_3^P \right) \\ Q &= Q_0 \left(\alpha_1^Q \cdot (\frac{V}{V_0})^2 + \alpha_2^Q \cdot (\frac{V}{V_0}) + \alpha_3^Q \right) \end{aligned} \quad (1)$$

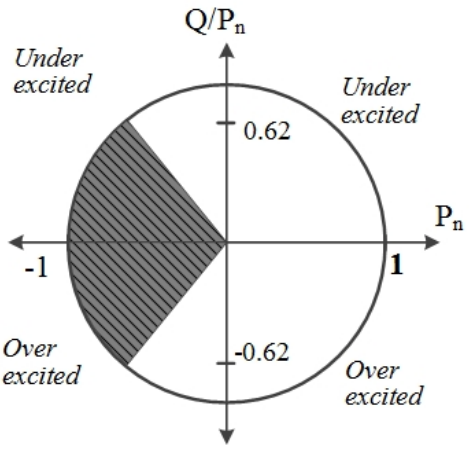

Fig. 2. Capability curve of PV system ($\leq$ 30 kW) set per the IEEE 1547 standard.

where P_0 and Q_0 are the active and reactive power consumptions by the load at nominal voltage V_0, while P and Q are active and reactive power consumptions during normal operating voltage V. Moreover, α_1^P, α_2^P, α_3^P are the active power coefficients for constant impedance, constant current, and constant power loads, and α_1^Q, α_2^Q, α_3^Q are the respective coefficients for the reactive power. It should be noted that those coefficients always sums up 1. Due to increased use of constant power loads in recent years [20], this study is performed with a reasonable assumptions of α_3^P and α_3^Q equals 1; that is to say the simulation is done per constant power load model.

C. BMES Model

The BMES is similar to the PV system while injecting power to grid (discharging) and similar to constant power load while drawing power from the grid (charging). Therefore, the BMES is also modeled as a dispatchable static generation or load that is capable of operating per the dispatched PQ signals. The capability curve of the BMES system is designed such that the overall PF at the PCC of the MGT stays $\pm$ 0.85 lead/lag or higher. However, the control strategy of the BMES is designed such that it operates at unity PF as long as there is no dispatch signal requiring an increase of reactive power injection/consumption. In this study, we modeled BMES such that charging and discharging power of BMES can be controlled between zero and its rated power.

D. Day-Ahead Forecasting

An auto regressive moving average (ARMA) is used for a day-ahead forecasting of PV production and feeder demand. Auto regression is modeled as a linear function of order p to describe a stochastic process and auto-correlations of past data, while moving average is modeled as a function of order q to estimate progress and trend on the direction of the stochastic function [10]. The forecasted parameter $y(t)$ is mathematically modeled as:

$$y(t) = \sum_{i=1}^{\rho} \phi_{\rho,i} y(t-i) + \sum_{k=1}^{q} \theta_{q,k} e(t-k) + e(t). \quad (2)$$

where p and q are the auto regressive and lagged forecast errors terms, $\phi_{p,i}$ and $\theta_{q,k}$ are parameters calculated based on ρ and q, and $e(t)$ is a zero-mean stationary white Gaussian noise. Moreover, $(t-i)$ and $(t-k)$ are backshift operators with delays i and k [21]. The ARMA model is constructed in MATLAB using a year of hourly PV production and load demand data.

III. Multi-Timescale Control Algorithm

This section presents details of the proposed multi-timescale control strategy to maximally deploy the benefits of BMESS. Particularly, a two-stage control approach is proposed, whereby BMES scheduling is done as a part of the first centralized scheduling stage and an adaptive update of the BMES operation is done as a part of the second real-time control stage. The schematic of the two-stage controls and their interaction is illustrated in Fig. 3 and described in detail in the following subsections.

A. Centralized Scheduling Stage

As mentioned in the preceding section, the first control stage is designed to proactively determine cost-optimal BMES operation schedules for the given combination of onsite PVs and loads. Mathematically, the control schedules are determined by minimizing the following objective function:

$$Min.\ C_i * \frac{1}{K_T} \sum_{i=1}^{N} (P_i^{BL} - P_i^{PV} + P_{i,Chg/Dsg}^{BT}) \cdot \delta t \quad (3)$$

where P_i^{BL} and P_i^{PV} are the forecasted values of base load and onsite PV generation, $P_{i,Chg/Dsg}^{BT}$ is the BMES charging-discharging schedules to be determined, C_i is the optimization coefficient, K_T is the normalization constant used to express time in hours, N is the total number of time slots, and i represents the time-slot index. If cost reduction is of key concern, C_i will be real-time electricity prices that is intended to reduce the total electricity costs, while if the demand reduction is of the key concern, C_i will be coefficients that should be a function of the loading conditions in the network. As our key target is to realize demand charge reduction through peak shaving, C_iś are derived from the load profile, particularly from forecasted daily load profiles, as follows:

$$C_i = \begin{cases} \in & P_{i,Net}^F = P_{min}^F \\ \frac{P_{i,Net}^F - P_{min}^F}{P_{Peak}^F - P_{min}^F} & P_{min}^F < P_{i,Net}^F < P_{Peak}^F \\ 1 & P_{i,Net}^F = P_{Peak}^F \end{cases} \quad (4)$$

such that net power ($P_{i,Net}^F$) equals the algebraic sum of the total demand and PV generation as follows:

$$P_{i,Net}^F = P_i^{BL} - P_i^{PV} \quad (5)$$

where P_{Peak}^F and P_{min}^F are the forecasted peak and minimum load periods for the next day. Moreover, $\in$ is the small positive number designed to force BMES for charging during low loading and/or high PV generation periods. In addition, higher values of C_i's during peak periods and/or low PV generation allows the BMES to discharge. This approach effectively helps to reduce the peak demands on the system. Moreover, it is

worth mentioning that the BMES charging/discharging is constrained by battery operational boundaries and desired demand regulation/reduction. At each time step ($\forall i = 1 : N$), the BMES is constrained by ramping rates, charging/discharging power, and state of charge (SOC) limits as follows:

$$\begin{aligned} 0 \leq P^{BT}_{i,Chg} < P^{BT}_{Max} \\ -P^{BT}_{Max} < P^{BT}_{i,Dsg} \leq 0 \end{aligned} \tag{6}$$

$$\begin{aligned} R^{Up} < \triangle P^{BT}_{i,Chg/Dsg} \leq P^{BT}_{Max} \\ R^{Dn} < \triangle P^{BT}_{i,Chg/Dsg} \leq P^{BT}_{Max} \end{aligned} \tag{7}$$

$$\begin{aligned} SOC_{Min} \leq SOC_i \leq SOC_{Max} \\ SOC_{i+1} = SOC_i + \frac{P^{BT}_{i,Chg/Dsg}\delta t}{BMES_{Cap}} \end{aligned} \tag{8}$$

where $P^{BT}_{n,Chg/Dsg}$ is the charging/discharging power of BMES that is subjected to its maximum rated power P^{BT}_{Max}, $R^{Up/Dn}$ is the allowable up/down ramping rate, SOC_i is the SOC of BMES at i^{th} time slot subjected to its minimum and maximum limits $SOC_{Min/Max}$, and $BMES_{Cap}$ is the BMES energy throughput. The first set of constraints (6) is designed to keep the charging/discharging of BMES within the allowable rated power, while the second set of constraints (7) prevents the BMES from ramping up/down for smaller values. Finally, the third set of constraints (8) is designed to keep the SOC within the predefined boundaries. Particularly, (7) and (8) are designed to keep BMES state of health in better conditions as well as to operate the BMES in the operating regimes that have higher efficiency. In addition, the BMES operation is constrained by the following equality constraints to ensure the consumer requirement/comfort.

$$SOC_{i=1} = SOC_{i=N} \tag{9}$$

where $SOC_{i=1}$ is the SOC of BMES at the beginning of the day and $SOC_{i=N}$ is the SOC at the end of the day. This constraint is designed mainly to keep the total energy content within the BMES to a constant value by the end of the day. The optimization is further subjected to constraint related to demand reduction targets as follows:

$$\begin{aligned} (P^{BL}_i - P^{PV}_i + P^{BT}_{i,Chg/Dsg}) \leq (\alpha + \epsilon_1) \cdot P^{F}_{Peak} \\ (P^{BL}_i - P^{PV}_i + P^{BT}_{i,Chg/Dsg}) \geq (\beta + \epsilon_2) \cdot P^{F}_{i,Net} \end{aligned} \tag{10}$$

where α and β are the user set targets for reducing the peak demand and filling the valley respectively, ϵ_1 and ϵ_2 are the relaxation variable, and P^{F}_{Peak} is the day-ahead forecasted peak load. This constraint gives an additional option for the BMES owner/user to set demand reduction targets if desired. For instance, if the consumer set targets do not meet (i.e., optimization does not converge), we relax the consumer set points and determine the best BMES schedules that gives convergence to the problem. In addition, to satisfy the user requirements, the optimization is further constrained by defining different blocks of time for charging and/or discharging. For instance, the BMES is prevented from discharging during certain time slots (e.g., low load, minimum price, or maximum PV generation) and vice versa.

$$P^{BT}_{i,Chg/Dsg} \geq 0 \quad t_1 < i < t_2 \tag{11}$$

$$P^{BT}_{i,Chg/Dsg} \leq 0 \quad t_3 < i < t_4 \tag{12}$$

where t_1 through t_4 are different time slots used to prevent/force BMES from charging or discharging at certain blocks of time. For instance, (11) forces the BMES to charge during the interval t_1 through t_2, while (12) forces the BMES to discharge during the time interval t_3 through t_4. It should be noted that multiple time periods can be set to direct BMES for charging/discharging per BMES owner preferences/requirements. If there are no such user preferences, constraints (11) and (12) can be discarded.

The optimization problem (3) is solved with constraints (6) through (12) using a dual-simplex solver in the optimization toolbox of MATLAB. The optimization results in optimal BMES schedules that reduce the peak demand, and in turn the demand charges for the BMES users. As electric utilities normally set demand charges based on the 15-minutes peak demand on a monthly basis, the performance of the proposed method should be evaluated either using monthly demand profiles or using a demand profile of the maximum demand day in a month. In this study, we have used the later approach to demonstrate the performance of the proposed control algorithm. However, it is worth mentioning that the proposed algorithm is generic and suits any time-frame without remarkable changes.

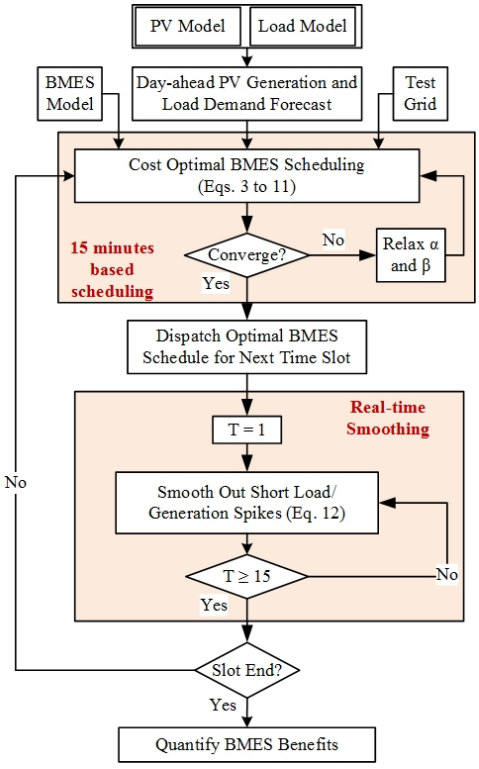

Fig. 3. High-level flow chart of the proposed algorithm.

B. Near Real-Time Adaptive Smoothing

As described in the preceding sections, the optimum BMES schedules are made on the basis of forecasted demand and PV generation profiles. Note that the forecasted onsite generation

can be tied with weather predictions and/or physics based models for better accuracy. Nevertheless, even though those schedules best serve for short-term planning purposes, they need additional adjustments in actual operation to cope with any uncertainties that may occur due to forecasting errors or any other unforeseeable events/contingencies. We proposed a second control stage that updates the BMES near real-time (1-minute resolution) to smooth out those contingencies and PV intermittencies. The key purpose is to compensate small spikes due to load/generation variations that may otherwise contribute to an increase in peak demand and demand charges. To do so, the BMES scheduled power ($P^{BT}_{Chg/Dsg}$) is updated every minute using the observed measurements. The updated control signal for BMES is computed as follows:

$$P^{BT,Upd}_{Chg/Dsg} = P^{BT}_{Chg/Dsg} + \frac{1}{K_T}\int_a^b (P^A_{Net} - P^F_{Net})\delta t \quad (13)$$

where $P^{BT,Upd}_{Chg/Dsg}$ is the updated BMES reference control signal computed through the difference between the actual measured and forecasted values of the net power, and a and b are the time interval in which the BMES schedules are updated. In our case, a and b are set to ensure the updates at every minute. This approach is very effective not only to smooth out the PV generation variabilities in smaller time resolution but also to follow the reference load signal that may stem from the local and/or upstream grid requirements. In the presented study, the real-time control algorithm is designed to keep the scheduled BMES operation intact. As depicted in Fig. 3, the BMES schedule gets updated periodically considering load/generation uncertainties and battery operating boundaries, and the coordination among two control stages is realized by using an intra-slot (every 15 minute) and inter-slot (near real-time) control mechanism.

IV. Implementation and Results

A 24-hours time sweep simulation is performed in a co-simulation environment using MATLAB and LabView. Particularly, all the computations, including optimization, are performed in MATLAB, while the time-series simulation, including near-real time control, is performed in LabView. The Performance of the proposed algorithm is demonstrated through three operating scenarios: low, medium, and high penetration of onsite PV. The economic performance is evaluated using the time-of-use (TOU) electricity price and demand charges taken from Southern California Edison's TOU-GS-2 Option B rate structure [22]. Particularly, the demand charge of 16.20/kW and TOU electricity price as illustrated Fig. 4 are used for the simulation purposes. The details of each simulation scenario and its effectiveness are described in the following subsections.

A. Scenario I: Low Penetration of Onsite PV

This scenario is primarily designed to emulate the effectiveness of the proposed method in a contemporary PV penetration scenarios; that is to say low PV penetration. In particular, the simulation is performed with approximately 15% PV penetration. According to the proposed algorithm, first, day ahead cost-optimal scheduling is done for the BMES for every 15-minutes time-slot by considering BMES operational boundaries, onsite PV generations, and load demands. Fig. 5a) illustrates the day-ahead forecasted values of demand, PV generation, and energy throughput to/from BMES. As demonstrated in Fig. 5b), the BMES is scheduled to discharge during a peak load period to reduce the peak demand and, in turn, demand charges. Similarly, the BMES is scheduled for charging during the periods when the feeder loading is lower. Looking from the TOU perspective (Fig. 4), it is seen that BMES is scheduled for charging during cheaper electricity price periods (e.g., late night and/or early morning) while scheduled for discharging during peak periods.

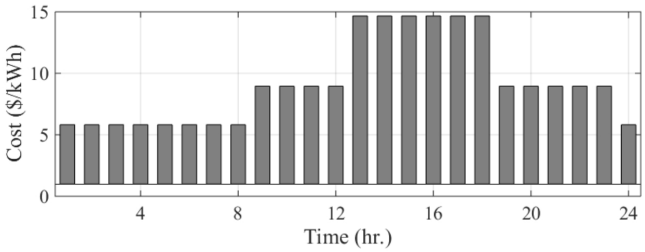

Fig. 4. TOU electricity price used in the simulation.

The optimal operational schedule from the first (scheduling) stage primarily forms a reference control signal to the second (near real-time) control stage. However, number of uncertainties (e.g., generation intermittencies, load spikes, and contingencies) that could occur during actual operation may deviate the BMES operational profiles from the cost-optimal schedules. As shown in the Fig. 5c), small variations ($+ve/-ve$) on load/generation occur quite frequently over the day. As those spikes may contribute to increase the peak demand, it is necessary to smooth them out in the smaller time frames. Near real-time control stage updates the BMES schedules every minute (1-minute resolution control) per observed intermittencies/variations in order to smooth out those deviations. It is seen in Fig. 5d) that BMES operates with a faster switching (charging-discharging) within a narrow range to keep the overall demand profile as scheduled. The near real-time control thus serves as a great tool for compensating the onsite PV generation and short load spikes.

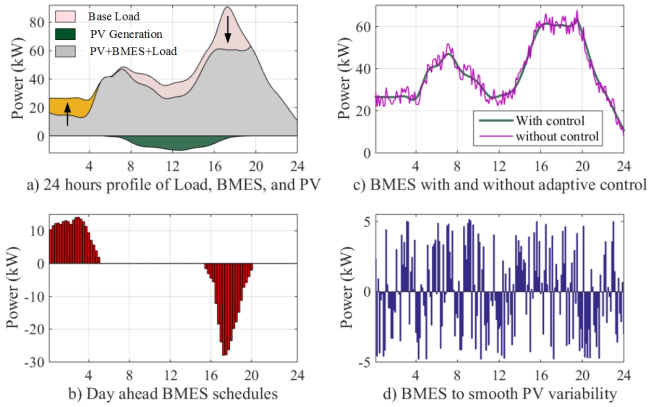

Fig. 5. Simulation results with low penetration of onsite PV.

B. Scenario II: Moderate Penetration of Onsite PV

Scenario II is performed to demonstrate the effectiveness of the proposed method with PV penetration in 5 to 10 years

from now; that is to say moderate PV penetration. In particular, the simulation is performed with approximately 30% PV penetration. In this case also, a day-ahead cost-optimal scheduling is first determined for the BMES considering its operational boundaries, onsite PV generations, and load demands. Fig. 6a) illustrate the 24-hours operating profiles of the microgrid system with and without PV and BMES, while Fig. 6b) illustrates the day ahead BMES schedules for the next 24-hours of the day. It can be seen that the BMES is scheduled to discharge during peak load period to reduce the demand charges, while scheduled for charging during the periods when the feeder loading is lower and PV generation is higher. The main take away from this scenario is that, unlike the previous case (LowPV), the BMES is scheduled for charging during the afternoon period when PV generation is relatively high.

Similar to the previous case, the near real-time control is activated with 1-minute of resolution to compensate any deviations on BMES optimal schedules made during the scheduling stage. As illustrated in Fig. 6c), the overall load looking from the upstream grid and/or utility looks pretty spiky. This would ultimately increase the peaks and woudl pose potential issues if the microgrid is participating in any regulating and balancing purposes. With the proposed 1-minute based control, all the spikes that may be encountered during the actual operation are compensated simply by making the reference load-following algorithm. It should be noted BMES should always be kept with a small (10% in our case) additional capacity to compensate those load and/or PV generation variability. One big difference compared to the low PV penetration case is that it results in more cost shaving and draws less power from the grid, thereby reducing the cost significantly as in Fig. 7.

C. Scenario III: High Penetration of Onsite PV

The key purpose of emulating Scenario III is to analyze how BMES owners get benefited using the proposed method with an increased penetration of onsite PV. The simulation is performed with a high (approximately 50%) PV penetration. The day-ahead cost-optimal BMES schedules, as illustrated in Fig. 8a) and Fig. 8a), are first determined using a forecasted scenario of onsite PV generation and load demand. It is demonstrated that the BMES is scheduled to discharge during a peak load period similar to the previous case, but charge during the afternoon when the PV has high generation. Even though the load from mid-night through early morning is quite

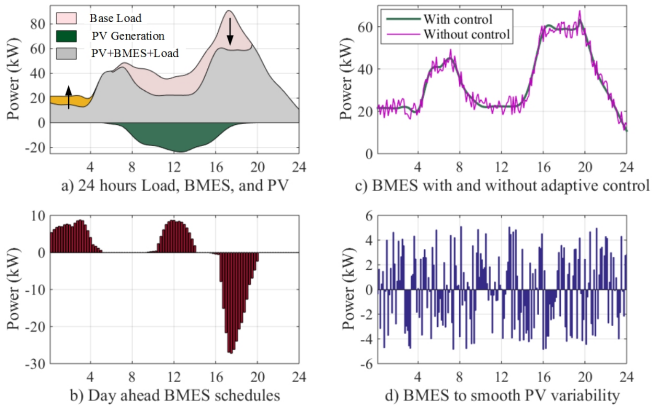

Fig. 6. Simulation results at moderate penetration of onsite PV.

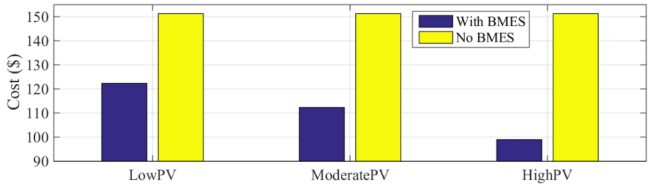

Fig. 7. Total cost (TOU+ demand charges) expressed on per day basis.

low, the BMES is scheduled to use the available PV generation efficiently by utilizing the PV power for charging. Similar to the previous case, any load and/or PV generation uncertainties that may stem from forecast errors and unexpected operating scenarios, as shown in Fig. 8c), are compensated for by forcing the BMES to capture those uncertainties. In particular, the control signal to the BMES is updated every minute considering the deviations shown in Fig. 8d). In addition to the peak shaving and load following, the proposed method can absorb PV over-generation and contributes positively to avoid grid over-voltage that may occur due to high PV penetrations.

As illustrated in Fig. 7, the total cost, which comprises the electricity cost as well as the demand charges, is significantly lower in the case of high onsite PV penetration compared to the other two cases. Moreover, it can be observed that the difference in total cost between with and without BMES is significantly high in each case, while the difference is highest in the case of high PV penetration. In fact, the total cost with BMES is significantly lower than that of the case without the BMES in all three scenarios.

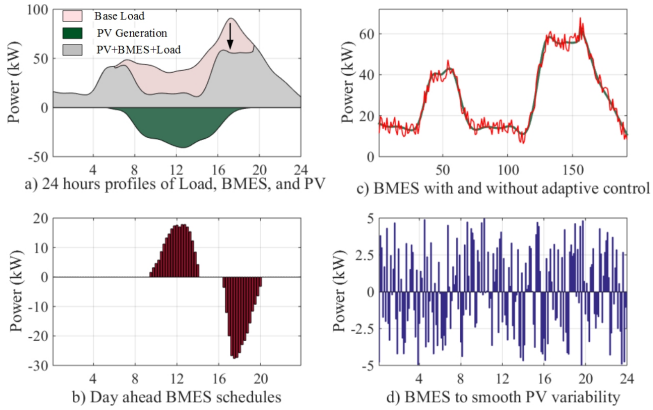

Fig. 8. Simulation results at high penetration of onsite PV.

V. Conclusion

We presented a multi-timescale control algorithm to exploit BMES benefits in reducing demand charge and smoothing onsite PV variability. First, the BMES schedule is determined to reduce system peak and in turn demand charges considering forecasted PV generation, electricity demand, and BMES operational boundaries. Those schedules form a reference control signal for the second stage, which smooths out load/generation spikes with shorter resolution (near real-time) control by enabling BMES to absorb those deviations. The performance of the proposed method is demonstrated through the 24-hours time sweep simulation for

three operating scenarios, namely low, moderate, and high penetration of onsite PV. The simulation results demonstrated that this is a simple yet sufficient method for peak shaving and demand charge reduction. More importantly, the near real-time control enables the proposed method to serve as an effective tool in load following and compensating the PV intermittency that may stem from forecast errors and/or rapid/random fluctuations on the loads.

REFERENCES

[1] J. Melcher, "Emergence of the Behind-the-Meter Energy Storage Market," *IEEE Smart Grid Newsletter*, Jan. 2016. [Online Available: http://smartgrid.ieee.org/newsletters/january-2016/emergence-of-the-behind-the-meter-energy-storage-market].

[2] Green Tech Media, "The future of energy storage is behind the meter," Nov. 2013. [Online Available: http://www.greentechmedia.com/articles/read/the-future-of-energy-storage-is-behind-the-meter].

[3] T. H. Mehr, M. A. S. Masoum, and N. Jabalameli, "Grid-connected lithium-ion battery energy storage system for load leveling and peak shaving," in *Proc. IEEE Australasian Universities Power Engineering Conference*, pp. 1-6, Sept. 2013.

[4] B. P. Bhattarai, M. Levesque, M. Maier, B. Bak-Jensen, and J. R. Pillai, "Optimizing electric vehicle coordination over a haterogeneous mesh network in a scaled down smart grid testbed," *IEEE Trans. on Smart Grid*, vol. 6, no. 2, pp. 784-794, Jan. 2015.

[5] M. J. E. Alam, K. M. Muttaqi, and D. Sutanto, "A controllable local peak shaving strategy for effective utilization of PEV battery capacity for distribution network support," in *Proc. IEEE Industry Application Society Annual Meeting*, pp. 1-8, Oct. 2014.

[6] B. P. Bhattarai, B. Bak-Jensen, J. R. Pillai, and M. Maier, "Demand flexibility from residential heat pump, in *Proc. IEEE Power and Energy Society General Meeting*, pp. 1-5, Jul. 2014.

[7] D. Wang, et. al., "A demand response and battery storage coordination algorithm for providing microgrid tie-line smoothing services," *IEEE Trans. on Sustainable Energy*, vol. 5, no. 2, pp. 476-486, Apr. 2014.

[8] B. P. Bhattarai, B. Bak-Jensen, J. R. Pillai, and P. Mahat, "Two-stage electric vehicle charging coordination in low voltage distribution grids," in *Proc. IEEE PES Asia-Pacific Power and Energy Engineering Conference*, pp. 1-5, Dec. 2014.

[9] A. Gholian, H. Mohsenian-Rad, and Y. Hua, "Optimal industrial load control in smart grid," *IEEE Transaction on Smart Grid*, Sept. 2015.

[10] B. P. Bhattarai, B. Bak-Jensen, J. R. Pillai, J. P. Gentle, and K. S. Myers, "Overvoltage mitigation using coordinated control of demand response and grid-tied photovoltaics," in *Proc. IEEE Conference on Technologies for Sustainability*, pp. 1-6, Jul. 2015.

[11] G. K. Venayagamoorthy, R. K. Sharma, P. K. Gautam, and A. Ahmadi, "Dynamic energy management system for a smart microgrid," *IEEE Transaction on Neural Networks and Learning Systems*, vol. 27, no. 8, pp. 1643-1656, Aug. 2016.

[12] Y. Kim, G. Del-Rosario-Calaf, and L.K. Norford, "Analysis and experimental implementation of grid frequency regulation using behind-the-meter batteries compensating for fast load demand variations," *IEEE Trans. on Power System*, Early access, May 2016.

[13] T. A. Nguyen, M. L. Crow, and A. C. Elmore, "Optimal sizing of a vanadium redox battery system for microgrid systems," *IEEE Trans. on Sustainable Energy*, vol. 6, no. 3, pp. 729-737, Jul. 2015.

[14] B. P. Bhattarai, B. Bak-Jensen, P. Mahat, J. R. Pillai, and M. Maier, "Hierarchical Control Architecture for Demand Response in Smart Grid Scenario, in *Proc. IEEE PES Asia-Pacific Power and Energy Engineering Conference*, pp. 1-6, Dec. 2013.

[15] Y. Wang, X. Lin, and M. Pedram, "Adaptive Control for Energy Storage Systems in Households with Photovoltaic Modules," *IEEE Trans. on Smart Grid*, vol. 5, no. 2, pp. 992-1001, Mar. 2015.

[16] Y. Wang, X. Lin, and M. Pedram, "A near-optimal model-based control algorithm for households equipped with residential photovoltaic power generation and energy storage systems," *IEEE Trans. on Sustainable Energy*, vol. 7, no. 1, pp. 77-86, Jan. 2016.

[17] B. P. Bhattarai, I. D. Mendaza, B. Bak-Jensen, J. R. Pillai, J. Gentle, and K. S. Myers, "Active control of thermostatic loads for economic and technical support to distribution grids, in *Proc. IEEE PES General Meeting*, pp. 1-5, Jul. 2016.

[18] Y. Kim, et. al., "Utilizing renewable energy resources by adopting DSM techniques and storage facilities," in *Proc. IEEE Conference on Communications*, June 2014.

[19] M. Ghamkhari and H. Mohsenian-Rad, "Optimal integration of renewable energy resources in data centers with behind-the-meter renewable generator," in *Proc. IEEE Conference on Communications*, pp. 3340-3344, Jun. 2012.

[20] B. P. Bhattarai, B. Bak-Jensen, P. Mahat, and J. R. Pillai, "Voltage Controlled Dynamic Demand Response, in *Proc. IEEE PES Innovative Smart Grid Technologies-Europe*, pp. 1-5, Oct. 2013.

[21] G. E. P. Box, G. M. Jenkins, and G. C. Reinsel, "Time series analysis, forecasting and control," 3rd ed., Englewood Cliffs, NJ: Prentice-Hall, 1994.

[22] J. Neubauer and M. Simpson, "Deployment of behind-the-meter energy storage for demand charge reduction," *Technical Report*, NREL/TP-5400-63162, January 2015.